

Mechanical properties of SiN_xC_y ceramic films prepared by plasma CVD

M. MORIYAMA

Nagano National College of Technology, Nagano City, 381 Japan

K. KAMATA, I. TANABE

Nagaoka University of Technology, Nagaoka City, 940-21 Japan

The mechanical properties of Si_3N_4 -SiC, SiN_x and SiC_y films prepared at a low temperature of 400°C by plasma chemical vapour deposition are reported. Microhardness, internal stress of the film and adhesive strength between the film and glass or stainless steel substrate were evaluated as principal mechanical properties. Microhardness was measured to be about 10 to 20 GPa dependent on the film composition in each system. Internal stress of the films on borosilicate glass substrates extensively varied from tensile to compressive with the film composition change from Si_3N_4 to SiC. Adhesive strength, as ascertained by the scratch test, was about 580 to 800 MPa for crown glass substrates, and about 210 to 310 MPa for 316 stainless steel substrates. It is pointed out that tensile stress in these films brought about more abrupt decreases of the adhesive strength than did compressive stress.

1. Introduction

Both silicon nitride (Si_3N_4) and silicon carbide (SiC) show excellent properties of strength, thermal stability, wear and corrosion resistance. They are very promising as structural ceramics because of their abundant existence on Earth. Generally, these materials are used as sintered compacts prepared by reaction sintering [1], pressureless sintering [2], and hot-pressing [3] methods.

However, an attractive method is to coat metals, glasses or other materials with ceramic films. The ceramic film coatings can provide the substrate materials with new and superior properties. The chemical vapour deposition (CVD) method, generally synthesizes various ceramic films with high density and strength at high deposition rates using chemical reaction [4, 5]. However, one of the major problems in utilizing this method over a wider industrial region is the thermal damage of the substrate materials at the reaction temperatures used. Recently, amorphous SiN_xC_y (Si_3N_4 -SiC, SiN_x and SiC_y systems) films were prepared using the plasma CVD method [6, 7]. By this method it is possible to prepare ceramic films on metals, glasses and even plastics at low temperatures (below 400°C) with the aid of active ions and radicals in r.f. plasma.

In addition to some mechanical properties, we have already reported the characteristics concerning infrared absorption spectra, optical band gap, refractive index and textures or microstructures for the prepared films [6–10]. It was concluded that silicon, nitrogen and carbon atoms in the film were uniformly distributed on an atomic scale (at least less than 1 nm diameter) [6, 7]. This paper investigates all the mechanical properties, including microhardness, internal

stress and adhesive strength as determined by the scratch test.

2. Experimental procedure

2.1. Preparation

The preparation of the films was performed using the charge-coupled plasma CVD apparatus under the conditions given in Table I [6, 7]. 10% SiH_4 (diluted with argon), NH_3 , C_2H_4 and H_2 were used as reaction gases. Table II shows the flow rates (F), flow-rate ratios (R) and compositions analysed by electron probe X-ray microanalysis (EPMA).

2.2. Measurement of mechanical properties

2.2.1. Microhardness and total stress

The microhardness of the films deposited on crown glass substrates was measured using a Vickers microhardness tester and evaluated as previously reported [8, 9]. The load of the indenter was fixed at 0.49 N, and the film thickness was kept above 5 μm in order to remove the influence of the substrate.

Internal stress in the film deposited on a thin circular borosilicate glass substrate of 15 mm diameter \times 0.153 mm thick was evaluated by measurement of the radius of curvature in elastic bending with a microstylus profilometer [8, 9].

Total stress is frequently used in order to express internal stress. Total stress, S , is given as a product of internal stress, σ_i , and film thickness, t_f

$$S = \sigma_i t_f \quad (\text{Nm}) \quad (1)$$

This total stress was used in this paper.

TABLE I Experimental conditions for plasma CVD apparatus

Deposition temperature	400 °C
Total gas pressure	66.7 Pa
r.f. frequency	13.56 MHz
r.f. power	100 W
Electrode spacing	30 mm
Electrode diameter	206 mm
Substrate	Crown glass Borosilicate glass, SUS-316

2.2.2. Adhesive strength

The adhesive strength between the film and substrate was measured by the scratch method [11]. As shown in Fig. 1, a Rockwell diamond indenter with the radius of 0.2 mm was used, and slid over the film with increasing indenter load. The film began to exfoliate from the substrate when the load reached a critical value. This critical load was detected by the rapid increase of acoustic emission (AE) signals from an AE sensor attached to the indenter holder. While adhesive force is frequently expressed by the critical load itself, it can be converted to adhesive strength (shearing stress between the film and the substrate) by the following equation [11]

$$\sigma_{ad} = \left(\frac{L_c}{\pi r^2 P - L_c} \right)^{1/2} P \quad (\text{Pa}) \quad (2)$$

where L_c is the indenter load (N), r the radius of the indenter tip (0.0002 m), P the reaction force per unit area acting from the substrate to the indenter, i.e. Brinell hardness (H_{BR}) of the substrate material. Crown glass ($H_{BR} = 3.90$ GPa) and 316 stainless steel (SUS-316; $H_{BR} = 1.96$ GPa) were used as substrate materials. Loading speed and sliding or scratching speed were 25 N mm^{-1} and 10 mm min^{-1} , respectively.

3. Results and discussion

3.1. Microhardness

Fig. 2 shows the relationships between the resulting Vickers microhardness and flow rate ratio of C_2H_4 (R_x) in Si_3N_4 -SiC films prepared by plasma CVD. The hardnesses of Si_3N_4 ($R_x = 0$, $\text{SiN}_{1.42}$ in Table II) and SiC ($R_x = 1.0$, $\text{SiC}_{1.04}$ in Table II) were about 20 and 12 GPa, respectively. The hardness of Si_3N_4 was considerably higher than that of SiC. The hardness of the mixed composition between Si_3N_4 and SiC was approximately equal to or somewhat lower than the above SiC value. It was revealed that the hardness of Si_3N_4 rapidly decreased with increasing SiC composition.

Fig. 3 shows the relationships between Vickers microhardness and atomic ratio of N/Si or C/Si in the binary systems of SiN_x and SiC_y . In both the systems, approximately stoichiometric composition of Si_3N_4 or SiC showed a maximum value in hardness. The microhardness of these films has already been reported in connection with other effects related to substrate materials and film thickness [9].

Table III shows the Vickers hardness values of both Si_3N_4 and SiC prepared by various methods. The hardness of Si_3N_4 prepared in this work is lower than that of amorphous and crystalline Si_3N_4 prepared by pyrolytic CVD, but comparable to, or somewhat higher than, that by reaction sintering or hot pressing at high temperatures (≥ 1400 °C). The Si_3N_4 film prepared shows a fairly high hardness in spite of the preparation at a low temperature of 400 °C. The hardness of SiC prepared by plasma CVD shows a relatively low value, being lower than half the values obtained by pyrolytic CVD and sputtering methods. This suggests a low binding strength of the bond between carbon and silicon. Therefore, the hardness of the SiC film obtained by plasma CVD might be

TABLE II Gas flow rates, F , gas flow rate ratios, R , and film compositions for plasma CVD $\text{Si}_x\text{N}_y\text{C}_z$ films

System	$F(10\% \text{SiH}_4\text{-Ar})^a$ (ml min ⁻¹)	$F(\text{NH}_3)$ (ml min ⁻¹)	$F(\text{C}_2\text{H}_4)$ (ml min ⁻¹)	$F(\text{H}_2)$ (ml min ⁻¹)	R_x^b	R_{nc}^c	Composition
Si_3N_4 -SiC	91	20	0	30	0	—	$\text{SiN}_{1.42}$
	91	16	4	30	0.20	—	$\text{SiN}_{1.23}\text{C}_{0.29}$
	91	12	6	30	0.33	—	$\text{SiN}_{0.90}\text{C}_{0.41}$
	91	8	8	30	0.50	—	$\text{SiN}_{0.65}\text{C}_{0.62}$
	91	4	9	30	0.69	—	$\text{SiN}_{0.40}\text{C}_{0.72}$
	91	0	10	30	1.0	—	$\text{SiC}_{1.04}$
SiN_x	95	12	0	30	0	1.26	$\text{SiN}_{0.84}$
	91	16	0	30	0	1.76	$\text{SiN}_{1.13}$
	90	17	0	30	0	1.89	$\text{SiN}_{1.20}$
	89	18	0	30	0	2.02	$\text{SiN}_{1.26}$
	87	20	0	30	0	2.30	$\text{SiN}_{1.37}$
	82	25	0	30	0	3.05	$\text{SiN}_{1.62}$
SiC _y	104	0	3	30	1.0	0.29	$\text{SiC}_{0.35}$
	103	0	4	30	1.0	0.39	$\text{SiC}_{0.56}$
	101	0	6	30	1.0	0.59	$\text{SiC}_{0.72}$
	95	0	12	30	1.0	1.26	$\text{SiC}_{1.07}$
	91	0	16	30	1.0	1.76	$\text{SiC}_{1.28}$
	87	0	20	30	1.0	2.30	$\text{SiC}_{1.38}$
Si	107	0	0	30	—	—	Si

^a $F(\text{SiH}_4) = 0.1 F(10\% \text{SiH}_4\text{-Ar})$.

^b Gas flow rate ratio of C_2H_4 : $R_x = F(\text{C}_2\text{H}_4) / [F(\text{C}_2\text{H}_4) + F(\text{NH}_3)]$.

^c $R_{nc} = [F(\text{C}_2\text{H}_4) + F(\text{NH}_3)] / F(\text{SiH}_4)$.

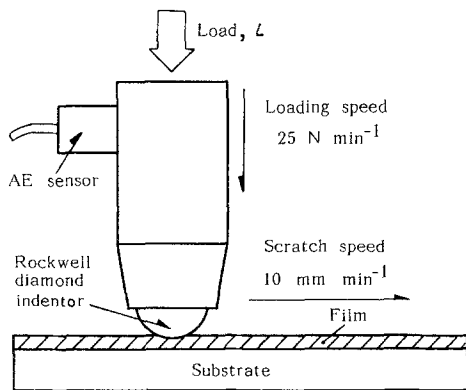


Figure 1 Measurement of adhesive strength by a scratch tester.

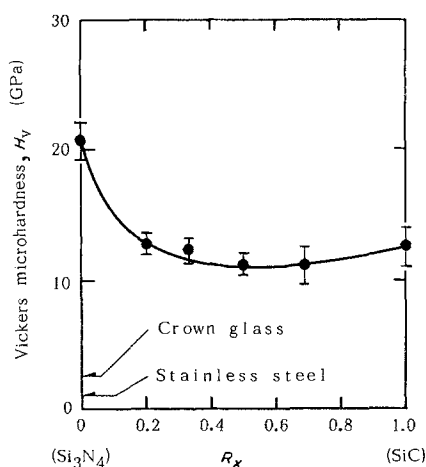


Figure 2 Vickers microhardness–flow rate ratio plots of C_2H_4 (R_x) for plasma CVD Si_3N_4 –SiC films. Indenter load 0.49 N, crown glass substrate, 5 μm film thickness.

improved by preparation under more progressive conditions.

3.2. Internal stress

Fig. 4 shows the relationships between the total stress and flow rate ratio of C_2H_4 (R_x) in the Si_3N_4 –SiC films prepared by plasma CVD. Total stress is given as a product of internal stress and film thickness as

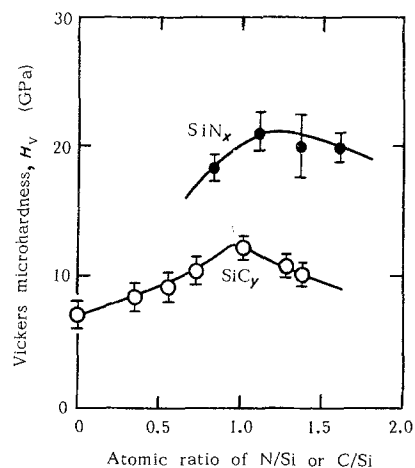


Figure 3 Vickers microhardness–atomic ratio plots of N/Si or C/Si for plasma CVD SiN_x and SiC_y films. Details as in Fig. 2.

mentioned above. The film thickness deposited on thin circular borosilicate glass substrates was kept constant at 1 or 5 μm . As shown in the figure, total stress (i.e. internal stress) varied monotonically from tensile to compressive as the film composition changed from Si_3N_4 to SiC. In the case of 1 μm thick, the total stress at Si_3N_4 ($R_x = 0$) composition was about 634 $N m^{-1}$ (tensile) and that at SiC ($R_x = 1.0$) composition was $-38.4 N m^{-1}$ (compressive). The internal stresses derived from the total stress were about 547 MPa (tensile) at Si_3N_4 and $-37.3 MPa$ (compressive) at SiC, respectively. For the 5 μm film thickness, the cracks due to the strong internal stress in the film occurred (\bullet). The tensile stress at $SiN_{0.65}C_{0.62}$ ($R_x = 0.5$) film (5 μm thick), at which cracks were beginning to occur, was about 159 MPa. This value is comparable to bending strength (103 to 255 MPa) or tensile strength (79 to 141 MPa) for the reaction-sintered Si_3N_4 [12]. Thus the tensile stress in the film is so high that cracks occur to relax the stress in the film. According to Goto *et al.* [13], the phenomenon of stress relaxation in Si_3N_4 with increasing carbon was reported in the Si_3N_4 –C system prepared by pyrolytic CVD. Generally, the compressive stress in the film is preferable so that cracks may not occur. In

TABLE III Vickers microhardness data for Si_3N_4 and SiC prepared by various methods

Materials	Preparation method	Preparation temp. ($^{\circ}C$)	Phase	Density ($kg m^{-3}$)	Hardness, H_v (GPa)	Reference
Si_3N_4	CVD	1300–1500	α	3180	30.4–37.2	[18]
	CVD	1100–1400	Amorphous	2600–2900	21.6–31.4	[18]
	Hot press	1850	$\alpha + \beta$	3120–3180	15.7–17.6	[19]
	PLS ^a	–	–	3100–3200	13.7–15.2	[20]
	RS ^b	–	α	2100	21.6	[18]
	RS ^b	–	β	2100	16.7	[18]
	Plasma CVD	400	Amorphous	–	20.2	This work
SiC	CVD	1500	β	–	33.0	[21]
	Sputter	370	Amorphous	–	35.3	[22]
	PLS ^a	–	–	3140–3180	27.4	[20]
	RS ^b	–	–	3100	24.5–34.3	[20]
	Plasma CVD	300	Amorphous	–	10.8–15.7	[23]
	Plasma CVD	400	Amorphous	–	12.2	This work

^a Pressureless sintering.

^b Reaction sintering.

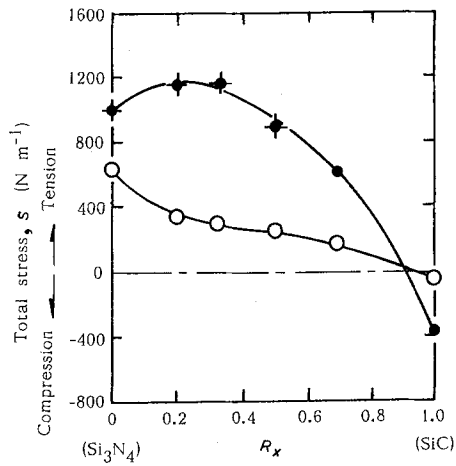


Figure 4 Total stress–flow rate ratio plots of C_2H_4 (R_x) for plasma CVD Si_3N_4 – SiC films. Film thickness: (●), 5 μm , (○) 1 μm , (◆) cracks on the films.

addition to this, when compressive stress acts in the film, the stress has been observed to increase greatly the flexural strength of the coated substrate. We succeeded in strengthening (by about twice) the flexural strength of the substrate when the SiC_y films ($\sim 5 \mu m$ thick) obtained by plasma CVD were coated on crown glass substrate ($\sim 1.2 mm$ thick) [10].

Fig. 5 shows the variation in the total stress with the atomic ratio of N/Si or C/Si in SiN_x and SiC_y films. In the case of the SiN_x film, the total stress varied discontinuously. The compressive stress was observed in ratios below ~ 1.2 and the tensile stress in those above ~ 1.2 . The colour of the films also changed from reddish brown (below ~ 1.2) to transparent (above ~ 1.2). Therefore, some structural change or transition might be caused in the vicinity of this atomic ratio. For the SiN_x film used as the passivation layer of IC circuits, the atomic ratio of N/Si of the layer is in the range 1.0 to 1.2 [14]. It is presumed that this atomic range is used in order to prevent the occurrence of cracks by inducing compressive stress in the films.

On the other hand, the compressive stress generally operated in the SiC_y films and increased with decreasing atomic ratio of C/Si. In addition, we have already reported that the internal stress in the films changes the crack length caused by the Vickers indenter and a certain relation exists between them [8].

It is reported that the internal stress is predominantly caused by the differences in the thermal shrinkage between the film and substrate through cooling from reaction temperatures [15]. Thermal stress, σ_t , is given by

$$\sigma_t = \frac{E_f}{1 - \nu_f} \int_{T_1}^{T_2} (\alpha_s - \alpha_f) dT$$

$$\approx \frac{E_f}{1 - \nu_f} (\alpha_s - \alpha_f) (T_2 - T_1) \quad (\text{Pa}) \quad (3)$$

where E_f , ν_f , α_f , α_s , T_1 and T_2 are Young's modulus (Pa), Poisson's ratio, thermal expansion coefficient of the film, thermal expansion coefficient of the substrate (borosilicate glass), the reaction temperature and the temperature at which the stress is measured (i.e. room

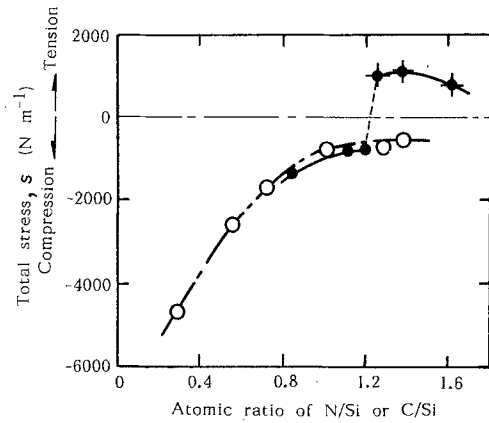


Figure 5 Total stress–atomic ratio plots of N/Si or C/Si for plasma CVD (●) SiN_x and (○) SiC_y films, for 5 μm film thickness; (◆) cracks on the films.

temperature), respectively. The stress in the films is tensile when $\sigma_t > 0$, and compressive when $\sigma_t < 0$. The condition for acquiring tensile stress in the film is $\alpha_s < \alpha_f$ and that for acquiring compressive stress is $\alpha_s > \alpha_f$ because $0 < \nu_f < 1$. The thermal expansion coefficient (α_s) of the borosilicate glass substrate is about $7.7 \times 10^{-6} \text{ } ^\circ\text{C}^{-1}$ (20 to 400 $^\circ\text{C}$). It is estimated by measurement of the total stress that the thermal expansion coefficient for the Si_3N_4 composition prepared by plasma CVD is above $7.7 \times 10^{-6} \text{ } ^\circ\text{C}^{-1}$ and that of SiC is lower than that value. According to Kern and Rosler [16], the thermal expansion coefficient of $Si_xN_yH_z$ ($y/x = 1.0$ to 1.2) film prepared by plasma CVD at 300 $^\circ\text{C}$ is the range 4 to $7 \times 10^{-6} \text{ } ^\circ\text{C}^{-1}$. The compressive stress in the SiN_x ($X < 1.2$) films in this work is consistent with the above results of thermal expansion coefficient, because α_s is greater than α_f .

Table IV shows the comparison of internal stresses in the SiN_x and SiC_y films obtained by pyrolytic CVD and plasma CVD methods. The internal stress in this experiment agrees roughly with the referred stresses prepared by plasma CVD, though these values of internal stress cannot be correctly compared with each other because of the difference in the detailed experimental conditions. It can be seen from Table IV that the stress induced by plasma CVD is considerably lower than that by pyrolytic CVD.

3.3. Adhesive strength

Fig. 6 illustrates a typical relationship between the exfoliation states of the films, AE count rate from the AE sensor, and the indenter load during scratching with the Rockwell diamond indenter. The indenter slid without exfoliation on the film under lower loads. However, exfoliation of the film started at a critical load with an abrupt and simultaneous increase in AE count rate. This increase in the AE count rate is understood to result from many AE signals originating from the exfoliations when the shearing stress induced by the diamond indenter exceeds the adhesive strength between the film and the substrate.

TABLE IV Internal stress data for SiN_x and SiC_y prepared by CVD and plasma CVD methods

Materials	Preparation	Film/subs.	Reaction temp. (°C)	Stress ^a (MPa)	Phase	Reference
SiN _x	CVD	SiN/Si	900	1200–1800	–	[16]
	Plasma CVD	SiN/Si	300	–100– – 800	Amorphous	[16]
	Plasma CVD	SiN/glass	300	–500	Amorphous	[16]
	Plasma CVD	SiN/Si	200–300	400–700	Amorphous	[14]
	Plasma CVD	SiN/glass	400	186–547	Amorphous	This work
SiC _y	CVD	SiC/W	1300–1500	690	β	[24]
	Plasma CVD	SiC/quartz	300	–20– – 200	Amorphous	[23]
	Plasma CVD	SiC/glass	400	–37– – 73	Amorphous	This work

^a Positive or negative values show tensile or compressive stresses, respectively.

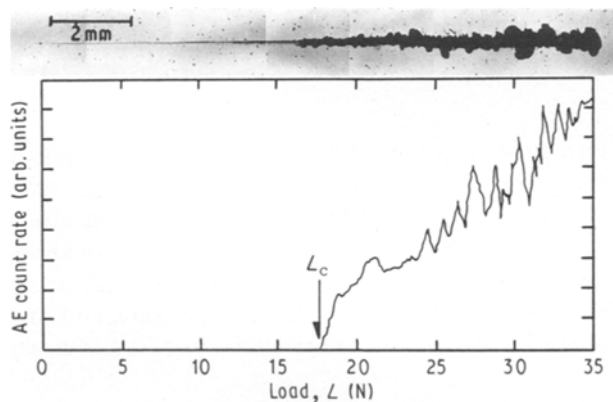


Figure 6 Variation of AE count rate with increasing indenter load, L , on scratch testing. View of the film exfoliation by the scratch is also shown. Specimen SiC_{1.07}, crown glass substrate, 1.0 μm film thickness.

Fig. 7 shows the variation of the critical load or adhesive strength with the film thickness in the Si₃N₄ films by plasma CVD. The adhesive strength lowered with increasing film thickness in the case of crown glass substrate. This lowering is considered to be responsible for the increase of tensile total stress in the Si₃N₄ films. With the increase in total stress, cracks occurred in the films, and the films were exfoliated easily by the loaded indenter. On the other hand, the critical load had little dependence on the film thickness in the case of SUS-316 substrates. The adhesive strength deposited on glass was higher than that on SUS-316. This difference in the adhesive strengths is considered to be due to first, the film on the glass can possess a strong Si–O bond between the film and substrate while that on SUS-316 does not have such strong bond, and second, the exfoliation of the films is easily promoted by the sinkage of the SUS-316 substrate (relatively soft materials) due to the depression of the indenter. In the case of the SiC films, only a little lowering of adhesive strength was observed with increasing thickness.

Fig. 8 shows the relationships between the critical load or adhesive strength and flow rate ratio of C₂H₄ (R_x) for the plasma CVD Si₃N₄–SiC films deposited on crown glass and SUS-316 substrates. The adhesive strength for the glass was about 740 MPa independent of the flow rate ratio (i.e. composition) at 1 μm thickness and that for the SUS-316 was about 210 to

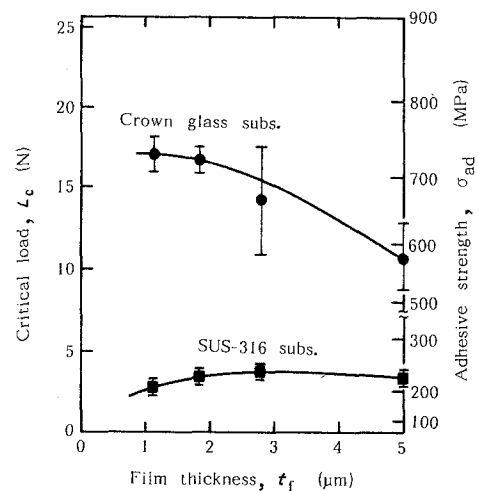


Figure 7 Variation of critical load, L_c and adhesive strength with film thickness for plasma CVD Si₃N₄ film. Films were deposited on crown glass and SUS-316 substrates.

310 MPa with change in flow rate ratio. In the case of 5 μm thick films, a maximum adhesive strength (792 MPa) for the glass was observed at the $R_x = \sim 0.5$. But, there was no maximum for the SUS-316, and adhesive strength was constant at about 240 MPa. The difference in the characteristics of adhesive strength between 1 and 5 μm film thickness for the glass substrate may be attributed mainly to the total stress in the film. In the case of 5 μm thick films, the adhesive strength varied with the change in total stress. The values of total stress for the borosilicate glass substrates are shown in Fig. 4 and the neutral point (i.e. the point at which total stress equals zero) is about 0.9 (R_x). For the crown glass substrate used to measure adhesive strength, the neutral point shifts to about 0.5 (R_x) as interpreted from the relationships between internal stress and crack length around the Vickers indentation [8]. The shift of the neutral point can be explained as a result of the difference in thermal expansion coefficients between the borosilicate ($7.7 \times 10^{-6} \text{ }^\circ\text{C}^{-1}$) and crown ($10 \times 10^{-6} \text{ }^\circ\text{C}^{-1}$) glass substrates [9]. The total stress varies extensively from tensile to compressive as the composition changes from Si₃N₄ to SiC. The maximum adhesive strength is shown at the point where total stress is zero, i.e. $R_x = \sim 0.5$. Therefore, the adhesive strength is lowered as the total stress (regardless of whether it is tensile or compressive) increases. The lowering in the

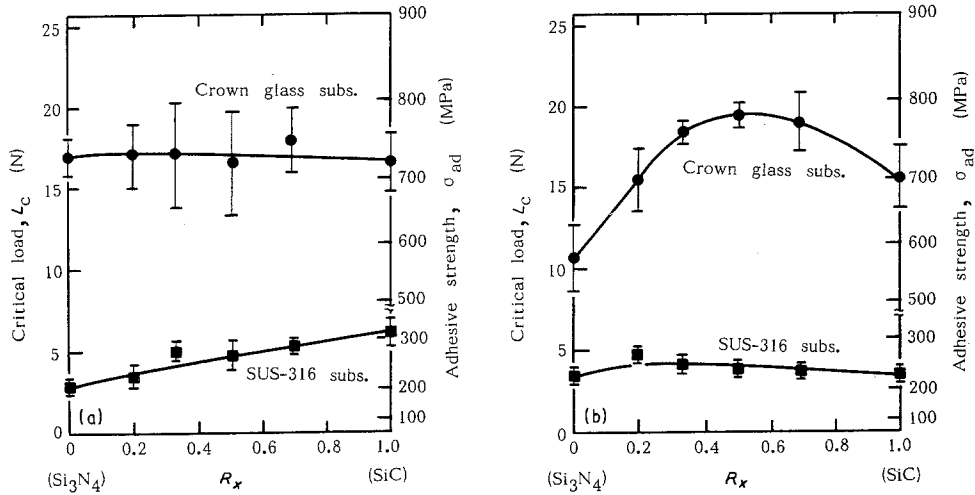


Figure 8 Critical load and adhesive strength-flow rate ratio plots of C_2H_4 (R_x) for plasma CVD Si_3N_4 -SiC films deposited on crown glass and SUS-316 substrates, for film thicknesses of (a) $1 \mu m$, (b) $5 \mu m$.

adhesive strength under tensile total stress (the Si_3N_4 composition) is larger than that under compressive stress (the SiC composition). This is probably because many cracks occur easily under tensile stress. In the case of $1 \mu m$ thick films, the total stress is relatively small because of its thinness. No variation of adhesive strength with film composition was observed.

Fig. 9 shows the variation of critical load and adhesive strength with the atomic ratio of N/Si for plasma CVD SiN_x films. The adhesive strength for the glass slowly decreased with the increasing atomic ratio of N/Si. This can be interpreted from the fact that compressive total stress acts in the low ratios of N/Si, and tensile total stress acts in the high ratios, as shown in Fig. 5.

Fig. 10 shows the variation of critical load and adhesive strength with atomic ratio of C/Si in SiC_y films. The adhesive strength for the glass decreased with increasing atomic ratio of C/Si in spite of the decrease in compressive total stress. This discrepancy between Figs 5 and 10 should be explained by another factor, besides the total stress. A great excess of silicon atoms without bonds exists in the film when the atomic ratio of C/Si is less than the stoichiometric composition (1.0). Adhesive strength increases by the

formation of strong Si-O bonds between excess silicon atoms in the film and oxygen atoms in the glass substrate. On the other hand, excess carbon atoms exist when C/Si is above 1.0. The excess carbon atoms might impair significantly the formation of strong Si-O bonds between the film and substrate, and thus might lower the adhesive strength. For SUS-316, the

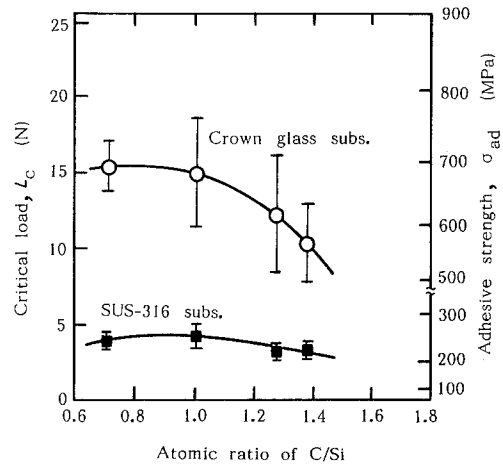


Figure 10 Critical load and adhesive strength-atomic ratio plots of C/Si for plasma CVD SiC_y films, for $5 \mu m$ film thickness.

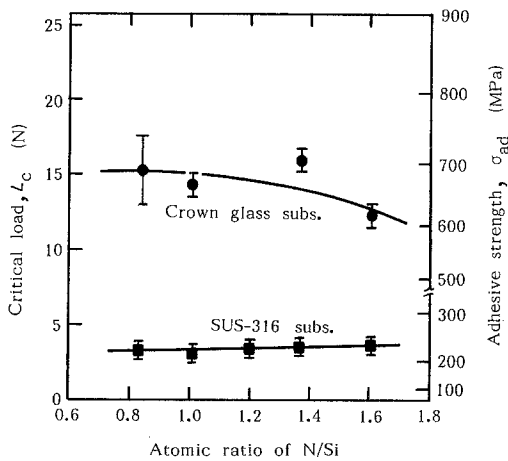


Figure 9 Critical load and adhesive strength-atomic ratio plots of N/Si for plasma CVD SiN_x films, for $5 \mu m$ film thickness.

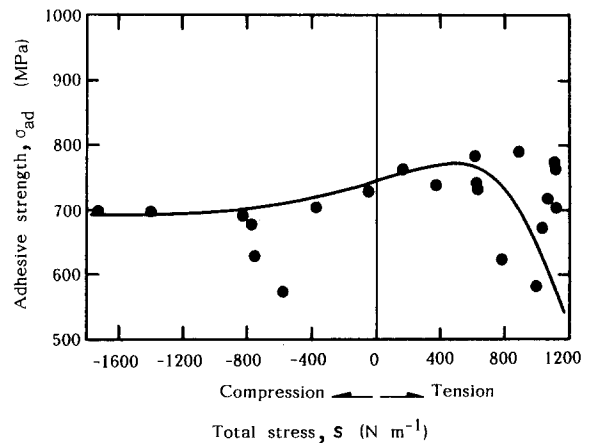


Figure 11 Relationships between the adhesive strength and total stress for plasma CVD SiN_xC_y films.

TABLE V Critical load, L_c , and adhesive strength, σ_{ad} , data for various ceramic films by scratch method

Film/subs.	Preparation method	Reaction temp. (°C)	Phase	Hardness, H_v (GPa)	Critical load, L_c (N)	Adhesive strength σ_{ad} (MPa)	Reference
Al ₂ O ₃ /glass	RS ^a	15–250	Amorphous	12–13	13–17	640–740	[17]
SiC/glass	RS ^a	250	Amorphous	22	12–19	620–780	[27]
TiN/WC	Ion plating	300–500	Crystal	22	39	–	[25]
TiC/WC	CVD	1000	Crystal	–	26	–	[26]
TiC/WC	Plasma CVD	800–900	Crystal	–	8–14	–	[26]
SiN _x /glass	Plasma CVD	400	Amorphous	18–20	12–16	620–720	This work
SiC _y /glass	Plasma CVD	400	Amorphous	8–12	10–15	580–700	This work
SiN _x C _y /glass	Plasma CVD	400	Amorphous	11–20	10–20	580–800	This work

^a Reactive sputtering.

adhesive strength was nearly independent of the ratio of C/Si.

In order to elucidate the relationships between adhesive strength and total stress, we investigated the correlation between them for all the specimens prepared as shown in Fig. 11. In the figure, total stress is plotted using the measured values for the borosilicate glass substrate. Therefore, the essential neutral point inevitably shifts to the right-hand side of the zero point for the crown glass substrate. This figure suggests that the largest adhesive strength is obtained when total stress is around zero. Furthermore, tensile total stress brings about an abrupt decrease in the adhesive strength between the film and substrate. On the other hand, compressive stress brings about only a small decrease in the adhesive strength.

Table V shows the critical load, L_c , and adhesive strength, σ_{ad} , data for various ceramic films as ascertained by the scratch method. The critical loads (or adhesive strengths) for SiN_xC_y, SiN_x and SiC_y films are comparable to those for Al₂O₃ or SiC films prepared by reactive sputtering and to TiC films prepared by plasma CVD.

4. Conclusions

The mechanical properties, such as microhardness, internal stress and adhesive strength, were investigated for the Si₃N₄–SiC, SiN_x and SiC_y films prepared by plasma CVD. The properties may be summarized as follows.

1. The Vickers microhardnesses of the Si₃N₄ and SiC composition films were about 20 and 12 GPa, respectively. The hardness of the mixed compositions between Si₃N₄ and SiC was approximately equal to that of SiC.

2. The stoichiometric compositions in SiN_x and SiC_y films showed maximum hardnesses.

3. The total stress (product of internal stress and film thickness) at the Si₃N₄ composition (1 μm thick) on borosilicate glass was about 634 N m⁻¹ (tensile) and that at the SiC composition was about –38.4 N m⁻¹ (compressive). The total stress in Si₃N₄–SiC films varied monotonically from tensile to compressive as the composition changed from Si₃N₄ to SiC.

4. The total stress in SiN_x films varied discontinuously from compressive to tensile at the N/Si ratio of

about 1.2 with increasing x. The compressive stress in SiC_y films increased monotonically with decreasing atomic ratio of C/Si.

5. The adhesive strength between the films and crown glass substrates was generally higher than that between the films and SUS-316 substrates. The adhesive strength for SUS-316 was about 210 to 310 MPa with a small dependence on film composition.

6. The adhesive strength of 1 μm thick films for glass substrates was constant at about 740 MPa regardless of the composition change of the films, while the maximum (792 MPa) was observed at about $R_x = 0.5$ (Si₃N₄:SiC = 1:1) for 5 μm thick films in the Si₃N₄–SiC system.

7. The adhesive strength in SiN_x and SiC_y films on glasses generally fell with increasing atomic ratio of N/Si or C/Si.

8. In these films, the maximum adhesive strength for glasses was observed when the compressive or tensile total stress was small or about zero. Moreover, it was concluded that the tensile stress brought about more abrupt decreases in the adhesive strength than the compressive stress.

Acknowledgements

The authors thank Dr Noriyuki Hayashi, Yuuji Maeda and Naoyoshi Aizawa for experimental assistance and useful discussions in this work.

References

1. H. M. JENNINGS, *J. Mater. Sci.* **18** (1983) 951.
2. F. F. LANGE and T. K. GUPTA, *J. Amer. Ceram. Soc.* **59** (1976) 537.
3. F. F. LANGE, *J. Mater. Sci.* **10** (1975) 314.
4. K. NIIHARA and T. HIRAI, *ibid.* **11** (1976) 593.
5. J. CHIN, P. K. GANTZEL and R. G. HUDSON, *Thin Solid Films* **40** (1977) 57.
6. K. KAMATA, Y. MAEDA and M. MORIYAMA, *J. Mater. Sci. Lett.* **5** (1986) 1051.
7. K. KAMATA, Y. MAEDA, K. YASUI and M. MORIYAMA, *Yogyo-Kyokai-Shi* **94** (1986) 12 (in Japanese).
8. K. KAMATA, N. AIZAWA and M. MORIYAMA, *J. Mater. Sci. Lett.* **5** (1986) 1055.
9. K. KAMATA, N. AIZAWA, Y. MAEDA and M. MORIYAMA, in "Proceedings of the World Congress on High Tech Ceramics", Milan, June 1986, edited by P. Vincenzini (Elsevier Science, Amsterdam, 1987) Part C, p. 2649.
10. M. MORIYAMA and K. KAMATA, *J. Mater. Sci. Lett.* **6** (1987) 1141.

11. P. BENJAMIN and C. WEAVER, *Proc. Roy. Soc.* **A254** (1960) 163.
12. J. W. EDINGTON, D. J. ROWCLIFFE and J. L. HENSHALL, *Powder Metall. Int.* **7** (1975) 82.
13. T. GOTO and T. HIRAI, *J. Mater. Sci.* **18** (1983), 3387.
14. A. K. SINHA, H. J. LEVINSTEIN, T. E. SMITH, G. QUINTANA and S. E. HASZKO, *J. Electrochem. Soc.* **125** (1978) 601.
15. D. S. WILLIAMS, *J. Appl. Phys.* **57** (1985) 2340.
16. W. KERN and R. S. ROSLER, *J. Vac. Sci. Technol.* **14** (1977) 1082.
17. M. MORIYAMA, K. KAMATA and I. TANABE, unpublished data, private communication, 1986.
18. K. NIIHARA and T. HIRAI, *J. Mater. Sci.* **12** (1977) 1243.
19. G. G. DEELEY, J. M. HERBERT and N. C. MOORE, *Powder Metall.* **8** (1961) 145.
20. M. ABE, M. KAWAI, T. KANNO and K. SUZUKI, in "Engineering Ceramics" (Gihoudou, Tokyo, 1984) p. 20 (in Japanese).
21. K. NIIHARA, *J. Amer. Ceram. Bull.* **63** (1984) 1160
22. K. WASA, T. NAGAI and S. HAYAKAWA, *Thin Solid Films* **31** (1976) 235.
23. H. YOSHIHARA, H. MORI and M. KIUCHI, *ibid.* **76** (1981) 1.
24. S. DUTTA, R. W. RICE, H. C. GRAHAM and M. C. MENDIRATTA, *J. Mater. Sci.* **15** (1980) 2183.
25. H. SUZUKI, H. MATSUBARA, A. MATSUO and K. SHIBUKI, *Funtai oyobi Funmatsu-Yakin (J. Jpn Soc. Powder and Powder Metall.* **32** (1985) 270 (in Japanese).
26. Y. DOI, A. DOI, M. TOBIOKA and A. IKEGAYA, *ibid.* **33** (1986) 413 (in Japanese).
27. K. KAMATA, N. SAITO, N. HAYASHI, I. TANABE and M. MORIYAMA, *J. Ceram. Soc. of Jpn* **98** (1990) 156 (in Japanese).

*Received 23 November
and accepted 1 December 1989*